Zero-Dead-Time Operation of Interleaved Atomic Clocks

G. W. Biedermann, K. Takase, X. Wu, L. Deslauriers, S. Roy, and M. A. Kasevich*

Physics Department, Stanford University, Stanford, California 94305, USA

(Received 26 April 2013; published 25 October 2013)

We demonstrate a zero-dead-time operation of atomic clocks. This clock reduces sensitivity to local oscillator noise, integrating as nearly $1/\tau$ whereas a clock with dead time integrates as $1/\tau^{1/2}$ under identical conditions. We contend that a similar scheme may be applied to improve the stability of optical clocks.

DOI: 10.1103/PhysRevLett.111.170802 PACS numbers: 06.30.Ft

In the 1950s atomic clocks revolutionized precision time keeping by locking a microwave source to an atomic resonance. Constant refinements improved the early fractional frequency stabilities near 10^{-10} [1] to the current levels below 5×10^{-16} [2]. In recent years, clocks based on optical transitions have progressed with a rapid pace, surpassing conventional microwave atomic clocks with frequency stabilities better than 10^{-17} [3–5]. Optical clocks are now beginning to perform tests of relativity [6] and constrain the possible time dependence of the fine structure constant [7].

Although these systems demonstrate unparalleled performance, they fail to realize their full potential. In the most stable clocks, the atomic linewidth is beyond the reach of current probe laser stability [8,9]. In general, this limits performance by forcing short interrogation times although the coherence of the atom far outlives that of the laser [10,11]. In this Letter we demonstrate a zero-dead-time technique in a microwave clock that can reduce these performance limitations as proposed in Ref. [12].

Atomic frequency standards often incorporate dead time in the interrogation of the atomic resonance. This interruption typically consists of state detection and initialization processes. Spurious drifts in the local oscillator (LO) frequency during the dead time are neither measured nor compensated. These drifts accumulate as an unknown phase or timing error. In an equivalent picture, the dead time effectively modulates the frequency discriminator sensitivity or feedback gain. This aliases high frequency LO fluctuations into the long term stability of the standard [12]. The magnitude of this, the Dick effect [13,14], depends strongly on the LO noise spectrum and the specifics of the clock interrogation. To assuage the Dick effect, microwave standards rely on LOs with outstanding short term stability and negligible contributions to the clock noise [15]. On the contrary, sufficient probe laser LOs for optical clocks are still pending. Alternatively, our approach addresses this inadequacy by interleaving two atomic clocks to constantly regulate the LO and eliminate the Dick effect completely.

To illustrate this technique we begin by calculating the cumulative phase error of an atomic clock based on a two-pulse Ramsey interrogation. In these clocks, a unit of time is defined by a prescribed number of cycles of a LO. For example, in a cesium fountain clock, a microwave oscillator is servo tuned to the $|F = 3, m_F = 0\rangle \rightarrow |F = 4, m_F = 0\rangle$ ground-state hyperfine resonance at $\omega_0 = 2\pi \times 9.2$ GHz. With the microwave field on resonance, the observable following a two-pulse $\pi/2$-$\pi/2$ Ramsey sequence is the atomic transition probability given by $P = \frac{1}{2}[1 + \cos(\Delta\phi)]$ where the quantity of interest

$$\Delta\phi = \phi^{\mathrm{LO}}(t+T) - \phi^{\mathrm{LO}}(t) - \omega_0 T = \int_t^{t+T} [\omega(t') - \omega_0] dt'. \quad (1)$$

Here ω_0 is the atomic resonance frequency, $\omega(t')$ is the frequency of the LO at time t', and T is the interrogation time.

In principle, the clock measurement detects the deviation of the LO phase with respect to the phase of the atom [16]. We therefore define

$$\delta\phi_n^{\mathrm{LO}} \equiv \phi_n^{\mathrm{LO}} - \omega_0 t_n, \quad (2)$$

where ϕ_n^{LO} is the LO phase at the nth $\pi/2$ pulse and t_n is the associated time stamp. Using Eq. (2) with Eq. (1)

$$\Delta\phi = \delta\phi_n^{\mathrm{LO}} - \delta\phi_{n-1}^{\mathrm{LO}}, \quad (3)$$

where $\delta\phi_n^{\mathrm{LO}}$ is associated with the second $\pi/2$ pulse in a given clock measurement pulse pair.

In an open loop mode, the cumulative LO phase as measured by a single clock (SC) is given by

$$\delta\Phi_{\mathrm{SC}} = \sum_{n=1}^{N} (\delta\phi_{2n}^{\mathrm{LO}} - \delta\phi_{2n-1}^{\mathrm{LO}}) + \sum_{i=1}^{N} \delta\phi_i^m. \quad (4)$$

In this equation $\delta\phi_i^m$ is the phase uncertainty associated with the quantum state measurement in the ith clock cycle,

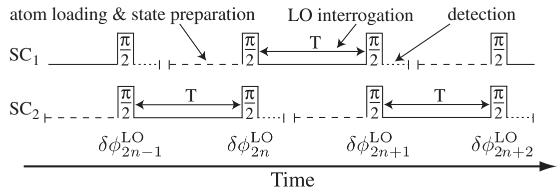

FIG. 1. Ramsey $\pi/2$ pulse timing diagram of a ZDT implementation of two clocks (SC_1 and SC_2). In each clock cycle the first (second) $\pi/2$ pulse of one clock coincides with the second (first) $\pi/2$ pulse of the other clock. Typical clock processes of detection and state preparation occur during the times between LO interrogation.

and N is the total number of cycles in the data. As expected, the performance of the clock is ultimately limited by the measurement noise. However, the single clock also ignores phase error during the dead time (DT) which accumulates as

$$\delta\Phi_{\rm DT} = \sum_{n=1}^{N}(\delta\phi_{2n+1}^{\rm LO} - \delta\phi_{2n}^{\rm LO}), \tag{5}$$

leading to the Dick effect. As illustrated in Fig. 1 our zero-dead-time (ZDT) approach uses a second clock to measure $\delta\Phi_{\rm DT}$.

We now calculate the cumulative phase error of the ZDT configuration. For this analysis we consider the specific case where $t_{n+1} - t_n = T$ for all n and thus the cycle time of each clock is $T_c = 2T$. The interleaved measurements are linked in time by synchronizing the first (second) $\pi/2$ pulse of one clock with the second (first) $\pi/2$ pulse of the other clock. When optimally implemented [17], the sum of the consecutive measurements cancels the phase noise in the shared pulses, such that only the phase from the first and last $\pi/2$ pulse in the data set contribute. Our experiment approximates this technique by using a square pulse shape. For two clocks, SC_1 and SC_2 with $N_{SC_1} = N_{SC_2} = N$, the cumulative phase is given by

$$\begin{aligned}\delta\Phi_{\rm ZDT} &= \delta\Phi_{SC_1} + \delta\Phi_{SC_2}\\ &= \sum_{n=1}^{N}(\delta\phi_{2n}^{\rm LO} - \delta\phi_{2n-1}^{\rm LO} + \delta\phi_n^{m_1})\\ &\quad + \sum_{n=1}^{N}(\delta\phi_{2n+1}^{\rm LO} - \delta\phi_{2n}^{\rm LO} + \delta\phi_n^{m_2})\\ &= \delta\phi_{2N+1}^{\rm LO} - \delta\phi_1^{\rm LO} + \sum_{n=1}^{N}(\delta\phi_n^{m_1} + \delta\phi_n^{m_2}).\end{aligned} \tag{6}$$

Here, $\delta\phi_n^{m_i}$ is the measurement error for clock i. This configuration concatenates $2N$ clock measurements, effecting a $2NT$ Ramsey interrogation time of the LO provided the measurement noise is negligible.

It is also illuminating to calculate the frequency uncertainty of the two schemes. In the case of stationary, white noise on the LO, the two-sample Allan deviation for the clock frequency measurements can be written as

$$\sigma_y(\tau) = \begin{cases} \frac{(N\sigma_{\Delta\phi}^2 + N\sigma_m^2)^{1/2}}{\omega_0}\frac{1}{\tau(T/T_c)} & \text{single clock}\\ \frac{(\sigma_{\Delta\phi}^2 + 2N\sigma_m^2)^{1/2}}{\omega_0}\frac{1}{\tau} & \text{ZDT.}\end{cases} \tag{7}$$

In these equations, $\sigma_{\Delta\phi} \equiv \sqrt{2}\langle(\delta\phi^{\rm LO})^2\rangle^{1/2}$ and $\sigma_m \equiv \langle(\delta\phi^m)^2\rangle^{1/2}$ are the rms noises in the clock output and measurement respectively, and the factor of $\sqrt{2}$ follows from the assumed independence of the two phase measurements in Eq. (4). For a single clock, adjacent measurements of $\Delta\phi$ are uncorrelated, so errors accumulate with a random walk, $\tau^{1/2}$, time dependence as do the quantum state measurement uncertainties. However, ZDT measurements are perfectly correlated such that the associated phase error is stationary. For clarity, we consider the case where the LO noise is characterized by white phase noise and the measurements by quantum projection noise. In systems of interest here, $\sigma_{\Delta\phi} \gg \sigma_m$ and we subsequently neglect measurement noise in our calculation. Using $N = \lfloor(\tau/T_c)\rfloor$ we find

$$\sigma_y(\tau) = \begin{cases} \frac{\sigma_{\Delta\phi}}{\omega_0 T}\sqrt{\frac{T_c}{\tau}} & \text{single clock}\\ \frac{\sigma_{\Delta\phi}}{\omega_0}\frac{1}{\tau} & \text{ZDT.}\end{cases} \tag{8}$$

The single clock averages as $1/\tau^{1/2}$ while ZDT averages as $1/\tau$ for $\tau < T_c/2(\sigma_{\Delta\phi}/\sigma_m)^2$. At longer times ZDT is limited by the measurement noise and averages as $\sigma_y(\tau) = \sigma_m/\omega_0(2/T_c\tau)^{1/2}$.

We demonstrate this concept with two microwave fountain clocks. A precision LO interrogates both clocks as shown in the system diagram of Fig. 2. The phase errors measured with each clock are combined and continuously

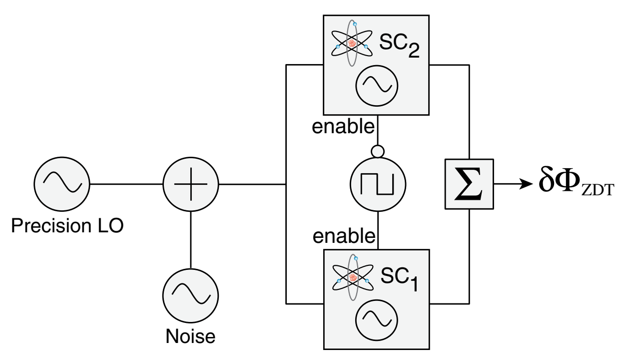

FIG. 2 (color online). High level schematic of our ZDT demonstration. Two identical atomic clocks, SC_1 and SC_2, alternately monitor the LO in the presence of an added phase noise. The combined outputs continuously track the resulting phase evolution.

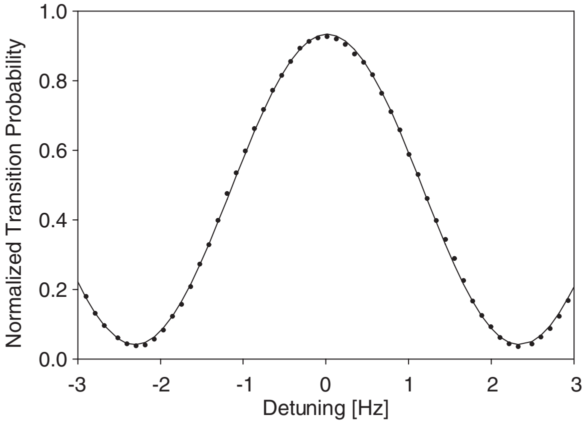

FIG. 3. Typical Ramsey clock fringe indicating the system noise floor. With $T = 215$ ms, the phase noise corresponds to a frequency stability of $1.8 \times 10^{-12}/\tau^{1/2}$, limited by noise in the LO distribution electronics.

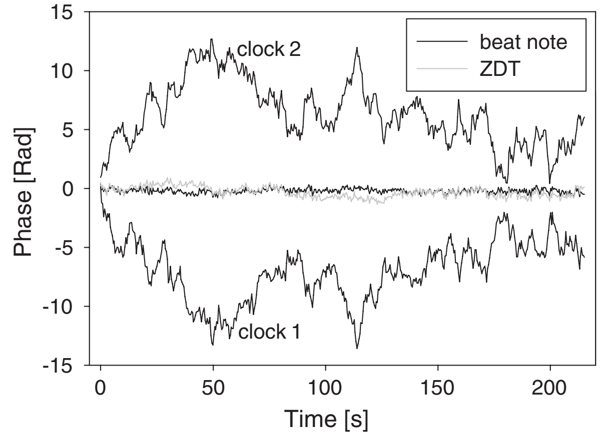

FIG. 4. Comparison of ZDT and conventional clock techniques. The cumulative beat-note phase is measured by comparing the noisy LO to the precision LO. The cumulative ZDT phase agrees with the cumulative beat-note phase and is bound at 440 mrad rms, whereas the cumulative single clock phase occasionally drifts by more than 10 rad.

monitor the phase evolution of the LO. To test this idea, we add a known noise source to the LO and compare the response of the single clock and ZDT approach.

Each individual clock sequence proceeds as follows. A 2.3 μK, 3 mm $1/e^2$ radius cloud of $\approx 10^7$ cesium atoms in the $6^2S_{1/2}$ $|F = 3, m_F = 0\rangle$ hyperfine ground state launches upward at 1.13 m/s using a moving-molasses technique. The cloud follows a 6.5 cm vertical fountain trajectory during which a microwave $\pi/2$-$\pi/2$ Ramsey sequence tuned to the $|F=3, m_F=0\rangle \rightarrow |F=4, m_F=0\rangle$ clock transition is applied to the atoms with an interrogation time of $T = 215$ ms. After the final pulse, the atoms fall into the detection region just below their point of origin. We determine the clock transition probability using simultaneous fluorescence detection of both states [18]. We choose the dead-time interval to match the interrogation time giving a repetition rate of $f_{\text{rep}} = 2.3$ Hz for each clock.

The clock noise floor is demonstrated by the Ramsey fringe shown in Fig. 3. Noise in the LO distribution electronics causes phase noise in the fringe at the level of $\sigma_m =$ 33 mrad per shot, giving a short-term fractional frequency uncertainty of $1.8 \times 10^{-12}/\tau^{1/2}$. The detection noise of each clock is negligible in this experiment. Using this as a baseline, we test our system by adding $\sigma_{\Delta\phi} =$ 300 mrad rms phase noise to the precision LO. To track this noise we monitor the zero crossings of a 1 kHz beat note between the noisy and unperturbed LO [19]. Because of the magnitude of the noise we account for the fringe contrast and slope nonlinearity when extracting phase values.

Figure 4 shows an example of the cumulative phase error of the noisy LO measured by our experiment. The single clock measures uncorrelated snapshots of the LO phase noise resulting in a random walk of the cumulative phase conforming to the expected value of $\sigma(t) = \sigma_{\Delta\phi}\sqrt{f_{\text{rep}} t} = 0.45\sqrt{t/\text{s}}$ rad rms. For comparison, over the entire data set the cumulative ZDT phase is limited to 440 mrad rms in contrast to the single clock which at times drifts by more than 10 radians. The residual drift of the ZDT output is driven primarily by uncorrelated noise between the two clocks due to the aforementioned LO distribution noise.

In Fig. 5 we compare the Allan deviation of both the single and ZDT clocks. The single clock reveals a frequency uncertainty slope of $1.3 \times 10^{-11}/\tau^{0.57}$, characteristic of white frequency noise. In contrast, the ZDT clock demonstrates a much improved slope of $6.2 \times 10^{-12}/\tau^{0.91}$, indicative of the applied white phase noise. For times larger than 50 seconds, Eq. (8) no longer holds as uncorrelated noise limits the slope to $1.2 \times 10^{-12}/\tau^{1/2}$.

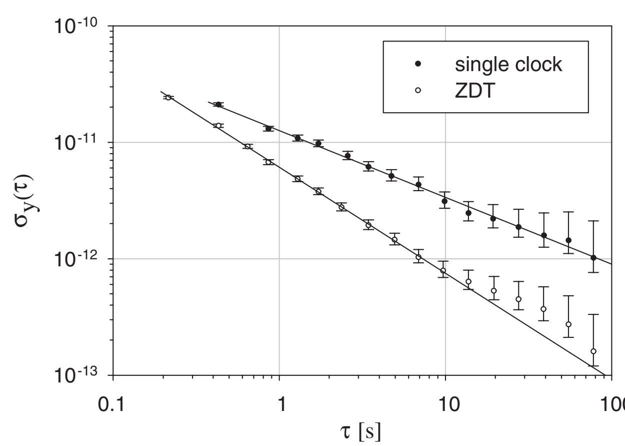

FIG. 5. Frequency uncertainty of conventional and ZDT clocks. In the first 10 seconds ZDT demonstrates $6.2 \times 10^{-12}/\tau^{0.91}$, characteristic of white phase noise while the single clock demonstrates $1.3 \times 10^{-11}/\tau^{0.57}$ due to the Dick effect.

In conclusion, we have demonstrated a ZDT operation of microwave atomic clocks which eliminates the Dick effect. We apply this method to a system with a noisy oscillator and show $1/\tau$ averaging in contrast to the $1/\tau^{1/2}$ averaging of conventional clocks with dead time. This technique can significantly ease the requirements on LO short term frequency stability in microwave and optical atomic clocks.

This work was supported by AFRL under Contract No. F19628-02-C-0096 and DARPA under Contract No. W911NF-06-1-0064.

*Kasevich@stanford.edu

[1] B. Guinot and E.F. Arias, Metrologia **42**, S20 (2005).
[2] T.E. Parker, Metrologia **47**, 1 (2010).
[3] T.L. Nicholson, M.J. Martin, J.R. Williams, B.J. Bloom, M. Bishof, M.D. Swallows, S.L. Campbell, and J. Ye, Phys. Rev. Lett. **109**, 230801 (2012).
[4] B.J. Bloom, T.L. Nicholson, J.R. Williams, S.L. Campbell, M. Bishof, X. Zhang, W. Zhang, S.L. Bromley, and J. Ye, arXiv:1309.1137.
[5] N. Hinkley, J.A. Sherman, N.B. Phillips, M. Schioppo, N.D. Lemke, K. Beloy, M. Pizzocaro, C.W. Oates, and A.D. Ludlow, Science **341**, 1215 (2013).
[6] C.W. Chou, D.B. Hume, T. Rosenband, and D.J. Wineland, Science **329**, 1630 (2010).
[7] T. Rosenband, D.B. Hume, P.O. Schmidt, C.W. Chou, A. Brusch, L. Lorini, W.H. Oskay, R.E. Drullinger, T.M. Fortier, J.E. Stalnaker, S.A. Diddams, W.C. Swann, N.R. Newbury, W.M. Itano, D.J. Wineland, and J.C. Bergquist, Science **319**, 1808 (2008).
[8] M. Bishof, X. Zhang, M.J. Martin, and J. Ye, Phys. Rev. Lett. **111**, 093604 (2013).
[9] M.M. Boyd, T. Zelevinsky, A.D. Ludlow, S.M. Foreman, S. Blatt, T. Ido, and J. Ye, Science **314**, 1430 (2006).
[10] H. Katori, Nat. Photonics **5**, 203 (2011).
[11] C.W. Chou, D.B. Hume, M.J. Thorpe, D.J. Wineland, and T. Rosenband, Phys. Rev. Lett. **106**, 160801 (2011).
[12] G.J. Dick, J.D. Prestage, C.A. Greenhall, and L. Maleki, in *Proceedings of the 22nd Precise Time and Time Interval (PTTI) Applications and Planning Meeting, Vienna, Virginia* (National Aeronautics and Space Administration, Washington, DC, 1990), pp. 487–508.
[13] G.J. Dick, J.D. Prestage, C.A. Greenhall, and L. Maleki, in *Proceedings of the 19th Precise Time and Time Interval (PTTI) Applications and Planning Meeting, Redondo, California* (National Aeronautics and Space Administration, Washington, DC, 1987), pp. 133–147.
[14] A. Quessada, R.P. Kovacich, I. Courtillot, A. Clairon, G. Santarelli, and P. Lemonde, J. Opt. B **5**, S150 (2003).
[15] R. Wynands and S. Weyers, Metrologia **42**, S64 (2005).
[16] N. Ramsey, *Molecular Beam Spectroscopy* (Clarendon, Oxford, 1956).
[17] To obtain uniform phase sensitivity during the pulses one may use amplitude modulation satisfying $g_1(t)+g_2(t)=1$ where $g_1(t)=\sin[(\pi/2t_p)\int_0^{t_p} a_1(t)dt]$ and $g_2(t)=\cos[(\pi/2t_p)\int_0^{t_p} a_2(t)dt]$, where a_i is the pulse amplitude of clock i [12].
[18] G.W. Biedermann, X. Wu, L. Deslauriers, K. Takase, and M.A. Kasevich, Opt. Lett. **34**, 347 (2009).
[19] D.W. Allan, J.H. Shoaf, and D. Halford, *Time and Frequency: Theory and Fundamentals*, edited by Byron E. Blair (National Bureau of Standards, Boulder, CO, 1974), Chap. 8, p. 151.